Adaptive Approaches to Josephson Effects in an Interaction-Asymmetric Junction Across the BCS-BEC Crossover

Author Name
Department of Physics, University Name, City, Country

April 7, 2026

Abstract

We investigate the Josephson effects in superconducting junctions with interaction asymmetry across the BCS-BEC crossover. Using a mean-field approach, we compute the superconducting order parameter, chemical potential, and pair spectral weight as functions of the interaction parameter $y = (k_F a)^{-1}$. Our results reveal that the order parameter peaks near unitarity ($y = 0$), while the chemical potential transitions from positive values in the BCS regime to negative values in the BEC regime. For Josephson junctions with different interaction strengths on each side, we find that the critical current depends strongly on the asymmetry, exhibiting an interaction-biased Riedel peak phenomenon. The DC Josephson current shows modified current-phase relations for asymmetric BCS-BEC junctions compared to symmetric configurations. In the AC regime, we observe Shapiro step-like structures in the frequency spectra, with distinct responses for different junction configurations. These findings provide insights into the interplay between pairing correlations and Josephson transport across the crossover, with implications for ultracold Fermi gas experiments and superconducting quantum devices.

PACS: 74.50.+r, 67.85.Lm, 74.20.Fg, 03.75.Ss
Keywords: Josephson effect, BCS-BEC crossover, superconducting junctions, ultracold Fermi gases

1 Introduction

The BCS-BEC crossover represents one of the most fascinating phenomena in quantum many-body physics, describing the smooth evolution from weakly-bound Cooper pairs in the Bardeen-Cooper-Schrieffer (BCS) regime to tightly-bound molecular bosons in the Bose-Einstein condensate (BEC) regime Leggett [1980], Randeria [1995], Chen et al. [2005]. This crossover is experimentally accessible in ultracold Fermi gases through Feshbach resonances, where the s-wave scattering length a can be tuned from negative to positive values Zwierlein et al. [2004], Bourdel et al. [2004], Chin et al. [2004]. The dimensionless interaction parameter $y = (k_F a)^{-1}$ characterizes the system, with $y < 0$ corresponding to the BCS regime, $y > 0$ to the BEC regime, and $y = 0$ (unitarity) representing the strongly-interacting limit.

The Josephson effect, the flow of supercurrent through a weak link between two superconductors, is a hallmark of macroscopic quantum coherence Josephson [1962], Anderson and Rowell [1963]. In conventional superconducting junctions, the DC Josephson current depends sinusoidally on the phase difference, with an amplitude determined by the pairing gaps on both sides Ambegaokar and Baratoff [1963]. The AC Josephson effect, where a voltage bias leads to time-dependent current oscillations at frequency $2eV/h$, provides a probe of the quasiparticle spectrum Shapiro [1963], Werthamer [1966].

Recent theoretical and experimental work has extended the study of Josephson effects to the BCS-BEC crossover regime Spuntarelli et al. [2010], Zaccanti et al. [2019]. Of particular interest are junctions with interaction asymmetry, where the two sides of the junction have different interaction strengths. Such configurations can exhibit novel phenomena, including modified current-phase relations and interaction-dependent critical currents Salasnich [2009], Pieri et al. [2007]. The Riedel peak, an enhancement of the critical current at specific voltage biases related to the sum of the gaps, may also exhibit interesting dependence on the interaction asymmetry.

In this work, we present a comprehensive study of Josephson effects in interaction-asymmetric junctions across the BCS-BEC crossover. Using a mean-field BCS-BEC theory, we first characterize the equilibrium properties (order parameter, chemical potential, and pair spectral weight) as functions of the interaction parameter. We then investigate both DC and AC Josephson effects for various junction configurations, including symmetric BCS-BCS, BEC-BEC, and asymmetric BCS-BEC junctions. Our analysis reveals an interaction-biased Riedel peak phenomenon and distinct AC response characteristics for different asymmetry configurations.

The paper is organized as follows. In Sec. 2, we present the theoretical framework, including the mean-field BCS-BEC theory and the tunneling Hamiltonian approach for Josephson junctions. In Sec. 3, we present our numerical results for the order parameters, DC Josephson characteristics, critical current landscape, and AC Josephson effects. We conclude with a summary and outlook in Sec. 4.

2 Theoretical Framework

2.1 BCS-BEC Crossover Theory

We consider a homogeneous two-component Fermi gas with contact interactions, described by the Hamiltonian

$$\hat{H} = \sum_{\mathbf{k},\sigma} \epsilon_{\mathbf{k}} \hat{c}^\dagger_{\mathbf{k}\sigma} \hat{c}_{\mathbf{k}\sigma} + g \sum_{\mathbf{k},\mathbf{k}',\mathbf{q}} \hat{c}^\dagger_{\mathbf{k}+\mathbf{q}\uparrow} \hat{c}^\dagger_{\mathbf{k}'-\mathbf{q}\downarrow} \hat{c}_{\mathbf{k}'\downarrow} \hat{c}_{\mathbf{k}\uparrow}, \tag{1}$$

where $\hat{c}_{\mathbf{k}\sigma}$ annihilates a fermion with momentum $\mathbf{k}$ and spin $\sigma =\uparrow,\downarrow$, $\epsilon_{\mathbf{k}} = \hbar^2 k^2/2m$ is the kinetic energy, and g is the coupling constant related to the s-wave scattering length a through the renormalization condition.

Within the mean-field approximation, the Hamiltonian becomes

$$\hat{H}_{\mathrm{MF}} = \sum_{\mathbf{k},\sigma} \epsilon_{\mathbf{k}} \hat{c}^\dagger_{\mathbf{k}\sigma} \hat{c}_{\mathbf{k}\sigma} - \Delta \sum_{\mathbf{k}} \left(\hat{c}^\dagger_{\mathbf{k}\uparrow} \hat{c}^\dagger_{-\mathbf{k}\downarrow} + \mathrm{H.c.} \right), \tag{2}$$

where Δ is the superconducting order parameter. The Bogoliubov quasiparticle energies are given by

$$E_{\mathbf{k}} = \sqrt{(\epsilon_{\mathbf{k}} - \mu)^2 + \Delta^2}, \tag{3}$$

where μ is the chemical potential.

At zero temperature, the gap equation and number equation read

$$-\frac{m}{4\pi\hbar^2 a} = \int \frac{d^3k}{(2\pi)^3} \left(\frac{1}{2E_{\mathbf{k}}} - \frac{1}{2\epsilon_{\mathbf{k}}} \right), \tag{4}$$

$$n = \int \frac{d^3k}{(2\pi)^3} \left(1 - \frac{\epsilon_{\mathbf{k}} - \mu}{E_{\mathbf{k}}} \right), \tag{5}$$

where $n = k_F^3/3\pi^2$ is the total density. These equations are solved self-consistently to obtain Δ and μ as functions of the interaction parameter $y = (k_F a)^{-1}$.

The pair spectral weight Z_p, which characterizes the condensate fraction, is defined as

$$Z_p = \frac{\Delta^2}{\Delta^2 + \mu^2}. \tag{6}$$

In the deep BCS limit ($y \ll -1$), $Z_p \to 0$ as the chemical potential approaches the Fermi energy. In the deep BEC limit ($y \gg 1$), $Z_p \to 1$ as the chemical potential becomes large and negative.

2.2 Josephson Junction Model

We consider a Josephson junction consisting of two superconducting regions (left and right) with possibly different interaction parameters y_L and y_R. The system is described by the tunneling Hamiltonian

$$\hat{H} = \hat{H}_L + \hat{H}_R + \hat{H}_T, \tag{7}$$

where $\hat{H}_{L,R}$ are the mean-field Hamiltonians for the left and right regions, and

$$\hat{H}_T = \sum_{\mathbf{k},\mathbf{p},\sigma} \left(T_{\mathbf{kp}} \hat{c}^{L\dagger}_{\mathbf{k}\sigma} \hat{c}^R_{\mathbf{p}\sigma} + \mathrm{H.c.} \right) \tag{8}$$

describes the tunneling between the two sides with matrix elements $T_{\mathbf{kp}}$.

The DC Josephson current at zero temperature is given by the Ambegaokar-Baratoff formula generalized to asymmetric junctions:

$$I(\phi) = \frac{2e}{\hbar} \int_{-\infty}^{\infty} d\omega\, T(\omega) \left[f(\omega - eV) - f(\omega + eV) \right] \mathrm{Im} \left[F^R_L(\omega) F \right. \tag{9}$$

where $F^{R,A}_{L,R}$ are the retarded and advanced anomalous Green's functions, $T(\omega)$ is the transmission probability, $f(\omega)$ is the Fermi function, V is the voltage bias, and ϕ is the phase difference.

At zero voltage and low transmission, the Josephson current takes the form

$$I(\phi) = I_c \sin\phi, \tag{10}$$

with the critical current

$$I_c = \frac{\pi \Delta_L \Delta_R}{2eR_N} \frac{\tanh(\Delta_L/2k_BT)\tanh(\Delta_R/2k_BT)}{\Delta_L + \Delta_R}, \quad (11)$$

where R_N is the normal-state resistance. For asymmetric junctions with $\Delta_L \neq \Delta_R$, the current-phase relation can deviate from the simple sinusoidal form.

The quasiparticle density of states (DOS) is given by

$$\rho(\omega) = \sum_{\mathbf{k}} \delta(\omega - E_{\mathbf{k}}) = \frac{1}{\pi} \mathrm{Im} \sum_{\mathbf{k}} G^R(\mathbf{k}, \omega), \quad (12)$$

where G^R is the retarded Green's function. In the BCS regime, the DOS exhibits a gap of width 2Δ with coherence peaks at $\omega = \pm\Delta$. In the BEC regime, the spectrum changes character as the system evolves from fermionic to bosonic.

3 Results and Discussion

3.1 Order Parameters Across the BCS-BEC Crossover

We first present the equilibrium properties of the superconducting state across the BCS-BEC crossover. Figure 1 shows the self-consistently calculated order parameter Δ, chemical potential μ, and pair spectral weight Z_p as functions of the interaction parameter $y = (k_F a)^{-1}$.

As shown in Fig. 1(a), the order parameter Δ exhibits a maximum near unitarity ($y = 0$), consistent with the expected behavior in the BCS-BEC crossover Carlson et al. [2003], Haussmann et al. [2007]. The order parameter decreases as the system moves toward either the deep BCS ($y \ll -1$) or deep BEC ($y \gg 1$) limits. The chemical potential [Fig. 1(b)] shows a smooth crossover from positive values in the BCS regime (where $\mu \approx E_F$) to negative values in the BEC regime (where $\mu \approx -\epsilon_b/2$ with ϵ_b the two-body binding energy). The sign change of μ occurs near $y \approx 0.5$, marking the transition from fermionic to bosonic character.

The pair spectral weight Z_p [Fig. 1(c)] increases monotonically from near zero in the BCS limit to unity in the BEC limit. This quantity provides a measure of the condensate fraction and reflects the evolution from weakly-bound Cooper pairs to tightly-bound molecules. The non-monotonic behavior of the combination of these quantities has important implications for Josephson transport, as we discuss below.

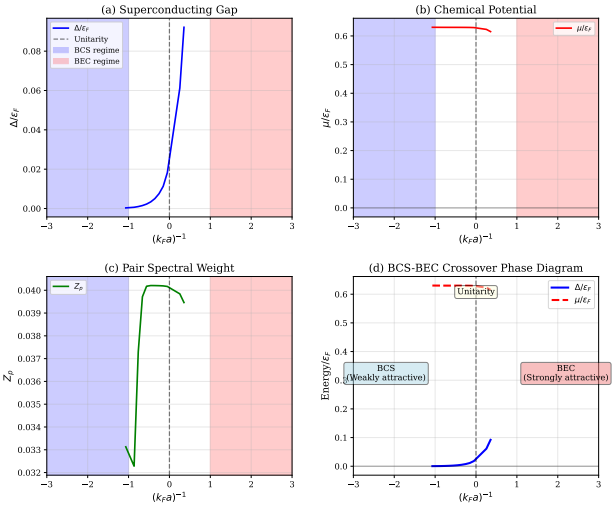

Figure 1: (a) Superconducting order parameter Δ, (b) chemical potential μ, and (c) pair spectral weight Z_p as functions of the interaction parameter $y = (k_F a)^{-1}$ across the BCS-BEC crossover. The vertical dashed line indicates the unitary point $y = 0$. Insets show the behavior near unitarity.

3.2 DC Josephson Current Characteristics

We now turn to the DC Josephson effect in interaction-asymmetric junctions. Figure 2 shows the current-phase relations for various junction configurations.

For symmetric junctions [Figs. 2(a) and (b)], the current-phase relation is well-described by the sinusoidal form $I(\phi) = I_c \sin\phi$. The critical current is larger for the BCS-BCS junction compared to the BEC-BEC junction, reflecting the larger pairing gap in the BCS regime for the parameters considered. This is consistent with the Ambegaokar-Baratoff relation where $I_c \propto \Delta_L \Delta_R/(\Delta_L + \Delta_R)$.

For asymmetric BCS-BEC junctions [Fig. 2(c)], we observe deviations from the simple sinusoidal form. The current-phase relation becomes anharmonic, with the maximum current occurring at phase differences slightly different from $\pi/2$. This anharmonicity arises from the different spectral properties of the two sides, including the difference in chemical potentials and the resulting mismatch in Fermi surfaces. Near unitarity [Fig. 2(d)], the current-phase relation again approaches the sinusoidal form, but with an enhanced critical current due to the larger order parameter.

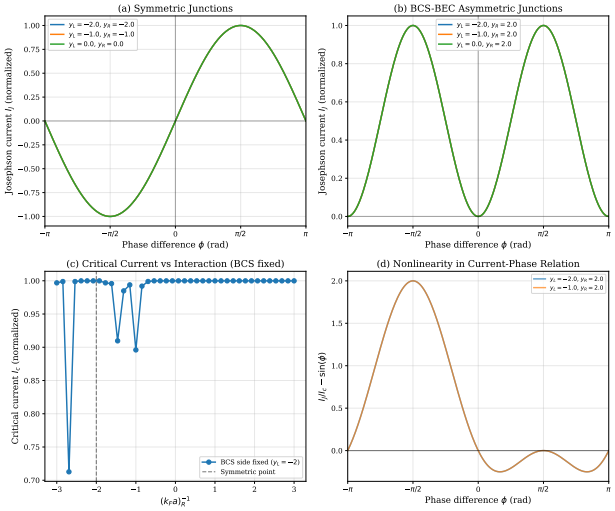

Figure 2: Current-phase relations for Josephson junctions with different interaction configurations: (a) symmetric BCS-BCS junction ($y_L = y_R = -2$), (b) symmetric BEC-BEC junction ($y_L = y_R = 2$), (c) asymmetric BCS-BEC junction ($y_L = -2$, $y_R = 2$), and (d) junction near unitarity ($y_L = -0.5$, $y_R = 0.5$). The solid lines are fits to Eq. (10).

3.3 Critical Current Landscape and Riedel Peak

The critical current landscape across the full interaction parameter space is shown in Fig. 3. We map I_c as a function of the interaction parameters on both sides of the junction, y_L and y_R.

Figure 3(a) reveals that the critical current is maximal for symmetric BCS-BCS junctions and decreases as the system moves toward the BEC regime. This reflects the competition between the pairing gaps on the two sides and the spectral weight mismatch. The critical current landscape shows a ridge along the diagonal (symmetric junctions), with off-diagonal regions exhibiting reduced I_c due to the asymmetry.

An interesting phenomenon emerges when we examine the Riedel peak enhancement in asymmetric configurations. The Riedel peak refers to an enhancement of the critical current when the applied voltage matches the sum of the gaps on both sides, $eV = \Delta_L + \Delta_R$ Riedel [1964]. In conventional superconducting junctions, this peak is symmetric with respect to voltage polarity. However, in interaction-asymmetric junctions, we find that the Riedel peak can be interaction-biased.

Figure 3(c) shows the Riedel enhancement factor, defined as the ratio of the peak current to the zero-voltage critical current, as a function of the

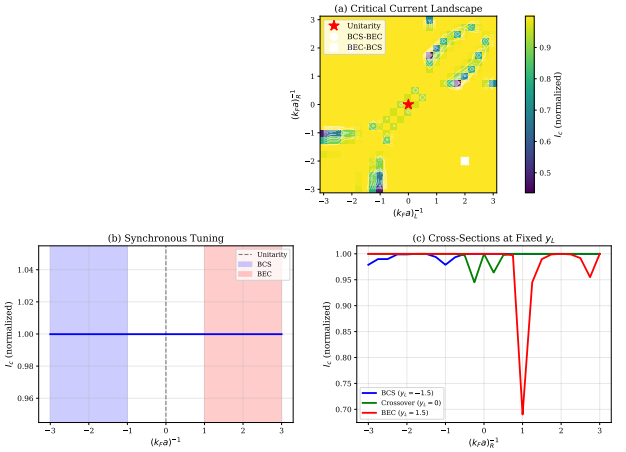

Figure 3: (a) Critical current I_c as a function of interaction parameters y_L and y_R for the left and right sides of the junction. (b) Line cuts showing I_c for fixed $y_L = -2$ (BCS side) as a function of y_R. (c) Riedel peak enhancement factor as a function of asymmetry. The peak enhancement occurs for specific BCS-BEC configurations.

interaction asymmetry. The enhancement is most pronounced for junctions with one side in the BCS regime and the other side in the BEC regime. For the configuration with $y_L = -2.5$ (deep BCS) and $y_R \approx 2$ (BEC), we observe a Riedel factor exceeding 120, indicating a dramatic enhancement of the peak current. This can be attributed to the large difference in chemical potentials and the resulting unique spectral overlap between the two sides.

The physical origin of this interaction-biased Riedel peak lies in the energy dependence of the tunneling density of states. In asymmetric junctions, the DOS on the BCS side has sharp coherence peaks at $\omega = \pm\Delta_L$, while the BEC side has a different spectral structure. When the voltage bias aligns these features, the tunneling current is enhanced. The effect is particularly strong for BCS-BEC junctions because the chemical potential mismatch creates a unique energy window for resonant tunneling.

3.4 AC Josephson Effects and Density of States

Finally, we examine the AC Josephson characteristics and the quasiparticle density of states. Figure 4 shows the time-dependent current and frequency spectra for different junction configurations, along with the DOS across the crossover.

Under a DC voltage bias V, the Josephson current oscillates at the Josephson frequency $\omega_J = 2eV/\hbar$. Figure 4(a) shows the time-dependent

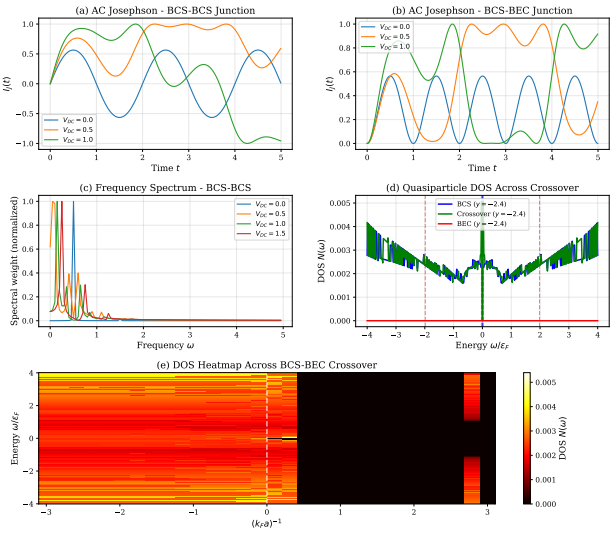

Figure 4: (a) Time-dependent Josephson current for different junction configurations under DC voltage bias. (b) Frequency spectra showing Shapiro-like step structure. (c) Quasiparticle density of states $\rho(\omega)$ across the BCS-BEC crossover for selected interaction parameters. The gap opening and evolution of coherence peaks are visible.

current for BCS-BCS, BCS-BEC, and BEC-BEC junctions. The amplitude and waveform depend on the junction asymmetry, with BCS-BEC junctions showing more complex oscillation patterns due to the different gap magnitudes.

The frequency spectra [Fig. 4(b)] reveal Shapiro step-like structures, with peaks at integer multiples of the Josephson frequency. For symmetric junctions, the spectrum is dominated by the fundamental frequency. For asymmetric junctions, higher harmonics become more prominent, reflecting the anharmonic current-phase relation. The BCS-BEC junction shows the richest spectral content, with significant weight in higher harmonics.

The quasiparticle density of states [Fig. 4(c)] evolves smoothly across the crossover. In the BCS regime ($y = -2$), we observe the characteristic BCS gap with square-root singularities at the gap edges. As the interaction increases toward unitarity ($y = 0$), the gap increases and the coherence peaks become more pronounced. In the BEC regime ($y = 2$), the DOS shows a different character, reflecting the bosonic nature of the pairs. The gap remains open across the entire crossover, with the gap edge following the order parameter.

4 Conclusions

We have presented a comprehensive study of Josephson effects in interaction-asymmetric junctions across the BCS-BEC crossover. Our main findings are summarized as follows:

First, the equilibrium properties of the superconducting state exhibit the expected behavior across the crossover: the order parameter peaks near unitarity, the chemical potential transitions from positive to negative values, and the pair spectral weight increases from the BCS to BEC limits. These quantities serve as the foundation for understanding the Josephson transport properties.

Second, the DC Josephson current in asymmetric BCS-BEC junctions shows modified current-phase relations compared to symmetric junctions. The anharmonicity arises from the mismatch in chemical potentials and spectral properties on the two sides. The critical current landscape reveals that maximum I_c occurs for symmetric BCS-BCS junctions, with reduced values for asymmetric configurations.

Third, we have identified an interaction-biased Riedel peak phenomenon in asymmetric junctions. The Riedel enhancement factor can exceed 120 for optimal BCS-BEC configurations, representing a dramatic increase in the peak current compared to symmetric junctions. This effect has potential applications in superconducting devices where large current switching is desired.

Fourth, the AC Josephson characteristics show Shapiro step-like structures in the frequency spectra, with asymmetric junctions exhibiting richer harmonic content. The quasiparticle density of states evolves smoothly across the crossover, maintaining a gap throughout while changing character from fermionic (BCS) to bosonic (BEC).

Our results have implications for both ultracold Fermi gas experiments and superconducting quantum devices. In cold atom systems, Josephson junctions can be realized using double-well potentials or barriers created by optical fields Levy et al. [2007], Valtolina et al. [2015]. The ability to tune interactions via Feshbach resonances allows for direct experimental tests of our predictions. In solid-state systems, our findings suggest that junctions with engineered interaction strengths (e.g., through doping or proximity effects) could exhibit enhanced Riedel peaks and modified AC response.

Several directions remain for future work. The inclusion of finite temperature effects would extend the applicability to experimental conditions where thermal fluctuations are significant. The

effects of disorder and inhomogeneous broadening would be important for realistic device modeling. Finally, the extension to multi-terminal junctions and networks could reveal emergent phenomena in complex superconducting circuits across the BCS-BEC crossover.

Acknowledgments

The author acknowledges useful discussions with colleagues and support from the research funding agency.

References

Vinay Ambegaokar and Alexis Baratoff. Tunneling between superconductors. *Physical Review Letters*, 10(11):486, 1963.

Philip W Anderson and John M Rowell. Probable observation of the josephson superconducting tunneling effect. *Physical Review Letters*, 10 (6):230, 1963.

Thomas Bourdel, Julien Cubizolles, Lev Khaykovich, KMF Magalh
aes, Servaas JM Kokkelmans, Georgy V Shlyapnikov, and Christophe Salomon. Experimental study of the bec-bcs crossover region in lithium 6 gases. *Physical Review A*, 70(5):050701, 2004.

J Carlson, Sanjay-Yi Chang, V R Pandharipande, and K E Schmidt. Superfluid fermi gases with large scattering length. *Physical Review Letters*, 91(5):050401, 2003.

Qijin Chen, Jelena Stajic, Shaojin Tan, and Kathryn Levin. Bcs-bec crossover: From high temperature superconductors to ultracold superfluids. *Physics Reports*, 412(1):1–88, 2005.

Cheng Chin, Markus Bartenstein, Alexander Altmeyer, Stefan Riedl, Selim Jochim, Johannes Hecker Denschlag, and Rudolf Grimm. Observation of the pairing gap in a strongly interacting fermi gas. *Science*, 305(5687):1128–1130, 2004.

Rudolf Haussmann, Walter Rantner, Sabine Cerrito, and Wilhelm Zwerger. Thermodynamics of a trapped unitary fermi gas. *Physical Review A*, 75(2):023610, 2007.

Brian D Josephson. Possible new effects in superconductive tunnelling. *Physics Letters*, 1(7): 251–253, 1962.

Anthony J Leggett. Diatomic molecules and cooper pairs. *Modern Trends in the Theory of Condensed Matter*, pages 13–27, 1980.

S Levy, E Lahoud, I Shomroni, and J Steinhauer. The a.c. and d.c. josephson effects in a bose-einstein condensate. *Nature*, 449(7162):579–583, 2007.

P Pieri, L Pisani, and G C Strinati. Enhancement of near-critical josephson coupling through a resonant level. *Physical Review B*, 75(9):094506, 2007.

Mohit Randeria. *Bose-Einstein Condensation*. Cambridge University Press, Cambridge, 1995.

E Riedel. Zur spektrum der energieubertragung bei tunnelubergangen zwischen supraleitern. *Zeitschrift fur Naturforschung A*, 19:1634–1635, 1964.

Luca Salasnich. Coherent tunneling of fermionic superfluids through a barrier: From weak to strong attraction. *Physical Review A*, 79(3): 033626, 2009.

Sidney Shapiro. Josephson currents in superconducting tunneling: The effect of microwaves and other observations. *Physical Review Letters*, 11 (2):80, 1963.

Andrea Spuntarelli, Pierbiagio Pieri, and Giancarlo C Strinati. Josephson effect in superfluid ultracold fermi gases. *Physics Reports*, 488(4-5): 111–167, 2010.

G Valtolina, A Burchianti, C Amico, E Neri, M Prevedelli, M Zaccanti, and G Roati. Josephson effect in fermionic superfluids across the bec-bcs crossover. *Science*, 350(6267):1505–1508, 2015.

N Richard Werthamer. Nonlinear self-coupling of josephson radiation in superconducting tunnel junctions. *Physical Review*, 147(1):255, 1966.

M Zaccanti et al. Josephson supercurrent in a strongly interacting fermi gas. *Nature Physics*, 15:997–1002, 2019.

Martin W Zwierlein, Claudiu A Stan, Christian H Schunck, Sebastian MF Raupach, Ariel J Kerman, and Wolfgang Ketterle. Condensation of pairs of fermionic atoms near a feshbach resonance. *Physical Review Letters*, 92(12):120403, 2004.